

# CFD Simulation of the Air Flow around a Car Model (Ahmed Body)

Senan Thabet\*, Thabit H. Thabit\*\*

\*University of South Wales, Cardiff, UK

\*\*Ninevah University, Mosul, Iraq

DOI: 10.29322/IJSRP.8.7.2018.p7979

<http://dx.doi.org/10.29322/IJSRP.8.7.2018.p7979>

**Abstract**— this paper describes the flow simulation focuses on the simulation around Ahmed body car with slant angle of  $40^\circ$ .

Computational Fluid Dynamics (CFD) is the proper approach to deal with these complicated equations and obtain the numerical solutions of these complicated flows equations.

The researchers conclude that CFD simulation has been carried out to investigate the flow characteristics over a model car (Ahmed Body). The aim was to calculate the aerodynamic coefficients from the CFD simulation and compared them with the available experimental data. The numerical results are agreed in decent way with experimental data.

**Keywords**— CFD, Ahmed Body, Air Flow, Simulation

## INTRODUCTION

This paper is investigating the flow simulation focuses on the simulation around Ahmed body car with a slant angle of  $40^\circ$  ( $CL=0.037$ ,  $CD=0.32$  &  $CM=0.036$ ).

From the literature review, slant angle of  $40^\circ$  is not the ideal angle for Ahmed car body. However, the literature shows that the proper angles lie between  $10-25^\circ$ .

In this analysis, a realizable  $k-\epsilon$  model with 2<sup>nd</sup> order accuracy. The flow governing equations within a CFD solver (ANSYS-Fluent) will be applied.

These are the continuity, momentum and energy equations. These equations are non-linear, partial differential equations (PDE's) and high orders, hence the analytical solution is impossible to obtain, (Saad & Ragavan, 2013). Computational Fluid Dynamics (CFD) is the proper approach to deal with these complicated equations and obtain the numerical solutions of these complicated flows equations (Kuzmin, 2010).

## CFD APPROACH AS DESIGN TOOL IN AUTOMOTIVE INDUSTRY

CFD simulations is an efficient tool in automatic industry used extensively for design. This allows the designers to obtain a quick and proper analysis before go ahead to the final

step. Recently, CFD approach has been adopted effectively within the automotive industry, with several new methods for car design (Smith, 2008).

CFD analysis in car industry is used in the determination of the applied forces and that of the vehicles wake during moving. CFD also is used to analyze the effect of wake on the vehicle's efficiency and capability in comparison with other cars (Thabet and Thabit, 2018). Figure 1 is an example that indicating how CFD can be used effectively in the context of vehicle design. It shows the flow paths (in terms of velocity magnitude) emanating from the wing-mirror structure of the Formula-1 racing car, and how it flows over the whole geometry.

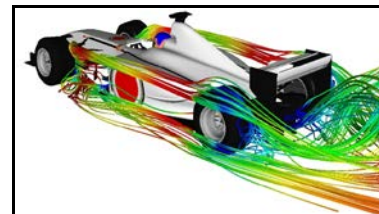


Fig. 1. CFD simulation for Formula-1 Racing Car (Smith, 2008)

In vehicle's industry, Ahmed Car Body is the standard model that can be used as validating case, in industry and CFD simulation (Davis, 2015). Ahmed Body is a generic car-type bluff body with a slant back has different angles from  $0 - 40$  degree. It is usually used as a benchmark test case for simulating the external aerodynamic flow characteristics over a car model (Hinterberger, et al., 2004).

## MAIN COMPONENTS IN A CFD SOLVER

CFD tool has three main components that is used to handle the object from the start point till analyzing the results (Thabit and Younus, 2018) These components can be summarized a follow:

### A. Pre-Processing:

This involves creating the geometry, computational domain

and meshing. Meshing is to discretising the computational domain into small control volumes, which are known as cells. The solution accuracy is a function of the number of generating cells in the computational domain.

**B. The Solver:**

This is the main part in the CFD simulation, where the flow governing equations will be discretised and solved.

**C. Post-processing:**

This is the final step in the CFD simulation process, which deals with extracting the important flow parameters such as velocity, density, pressure and forces. The simulation results will be compared to the experimental data and other numerical simulations.

**AIMS & OBJECTIVES**

The aim of this assignment is to perform a mathematical and CFD analysis on the flow over Ahmed Body and compared the numerical results with the available experimental data. The study will be carried out using both Solidworks and ANSYS software to create the geometry and obtain the numerical solution, respectively.

**PROBLEM ASSUMPTIONS**

From the given data in the assignment, the follow points will be assumed during the CFD simulation of the present problem. There is no heat transfer between the flow and the geometry. Air velocity at the inlet section is constant value during the solution. All the object boundaries will be dealt as walls with no slip shear condition. Because the Mach number is less than 0.3, hence the flow will be assumed as incompressible flow.

**NUMERICAL METHODS:**

**D. Governing Equations:**

To simulate the incompressible flow, Navier-Stokes equations for this flow type will be solved. The form of these equations based on the flow assumption follows:

**1) Continuity Equation:**

$$\frac{\partial \rho}{\partial t} + \frac{\partial(\rho u)}{\partial x} + \frac{\partial(\rho v)}{\partial y} + \frac{\partial(\rho w)}{\partial z} = 0$$

For an incompressible flow

$$\frac{\partial \rho}{\partial t} = 0, \quad \nabla \cdot (\rho \vec{V}) = 0$$

Thus;

$$\frac{\partial u}{\partial x} + \frac{\partial v}{\partial y} + \frac{\partial w}{\partial z} = 0$$

Where,

$$\rho = C, \quad \nabla \cdot \vec{V} = 0$$

**2) N-S Equations:**

**a) X-direction component:**

$$\frac{\partial(\rho u)}{\partial t} + \nabla(\rho u V) = -\frac{\partial p}{\partial x} + \frac{\partial \tau_{xx}}{\partial x} + \frac{\partial \tau_{yx}}{\partial y} + \frac{\partial \tau_{zx}}{\partial z} + \rho f_x$$

**b) Y-direction component:**

$$\frac{\partial(\rho v)}{\partial t} + \nabla(\rho v V) = -\frac{\partial p}{\partial y} + \frac{\partial \tau_{yx}}{\partial x} + \frac{\partial \tau_{yy}}{\partial y} + \frac{\partial \tau_{zy}}{\partial z} + \rho f_y$$

**c) Z-direction component:**

$$\frac{\partial(\rho w)}{\partial t} + \nabla(\rho w V) = -\frac{\partial p}{\partial z} + \frac{\partial \tau_{zx}}{\partial x} + \frac{\partial \tau_{yz}}{\partial y} + \frac{\partial \tau_{zz}}{\partial z} + \rho f_z$$

**E. Boundary Conditions**

The following boundary conditions are applied during the solution in ANSYS-Fluent.

- Velocity-inlet BC: Inlet plane.
- Symmetry BC: Enclosure surfaces (no-slip conditions).
- Walls BC: Road and object surfaces.
- Pressure-outlet BC: Outlet plane.

**F. Flow Inlet Parameters:**

$$\mu = 1.789 \times 10^{-5} \text{ kg/m.s.}$$

$$\nu = 15.13 \times 10^{-6} \text{ m}^2/\text{s.}$$

$$\rho = 1.225 \text{ kg/m}^3.$$

$$V = 40 \text{ m/s.}$$

$$Re = 768,000 \text{ (based on object's height).}$$

$$I \leq 0.25\%$$

**G. Car Model Geometry:**

Figure 2 shows the layout of the geometry provided in the assignment cover sheet for Ahmed Body Car with a slant angle  $\phi$  equals to  $40^\circ$ . From the figure below, the horizontal length covered by the slant (L) and its height (H) can be calculated as follow:

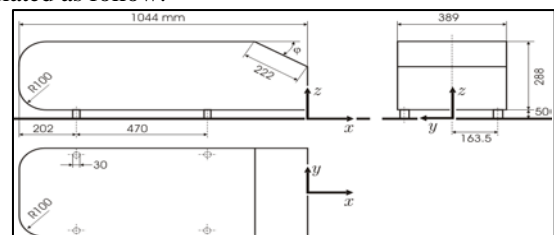


Fig. 2. Layout of Ahmed Body

$$\cos \phi = \frac{\text{horizontal distance covered by slant (L)}}{\text{Slant length}}$$

$$\cos 40 = \frac{L}{222}$$

$$L = 170.06 \text{ mm}$$

Hence,

$$x = 1044 - 170.06 = 873.94 \text{ mm}$$

$$\sin \phi = \frac{\text{vertical distance covered by slant}}{\text{slant length}}$$

$$\sin 40 = \frac{H}{222}$$

$$H = 142.70 \text{ mm}$$

Hence,

$$z = 288 - 142.70 = 145.30 \text{ mm}$$

Using Solidworks software, CAD model for Ahmed Body is created and exported with IGS extension to be dealt in ANSYS Workbench. Figure 3 shows the Car Model Geometry for Ahmed Body.

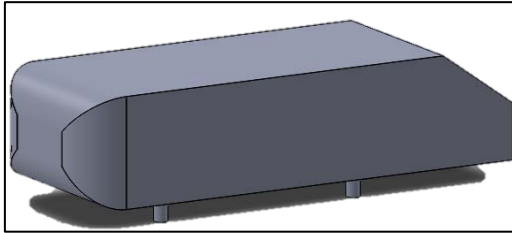


Fig. 3. Ahmed Car Body CAD Model

**H. Computational Domain:**

ANSYS software tools (workbench, Design Modular, Meshing tool & Fluent solver) are used to carry out the flow simulation.

Figures 4 and 5 show a screenshot during preparing the solution and creating the enclosure by using ANSYS workbench, and Design Modular, respectively.

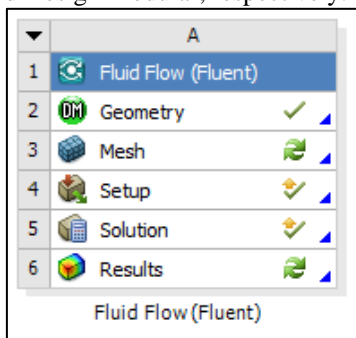


Fig. 4. Fluent Solver

Details of Enclosure1	
Enclosure	Enclosure1
Shape	Box
Number of Planes	2
Symmetry Plane 1	YZPlane
Symmetry Plane 2	ZXPlane
Model Type	Full Model
Cushion	Non-Uniform
<input type="checkbox"/> FD1, Cushion +X value (>0)	1044 mm
<input type="checkbox"/> FD2, Cushion +Y value (>0)	706 mm
<input type="checkbox"/> FD3, Cushion +Z value (>0)	1000 mm
<input type="checkbox"/> FD4, Cushion -X value (>0)	1044 mm
<input type="checkbox"/> FD5, Cushion -Y value (>0)	0 mm
<input type="checkbox"/> FD6, Cushion -Z value (>0)	4176 mm
Target Bodies	All Bodies

Fig. 5. Enclosure Option Box

Figure 6 shows the Car Model with the enclosure created in Design Modular.

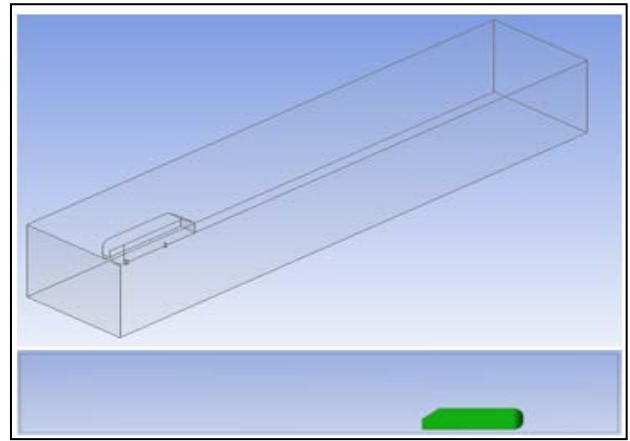


Fig. 6. Geometry and Enclosure

Figure 7 shows the Boolean operation on Ahmed Body and fluid body.

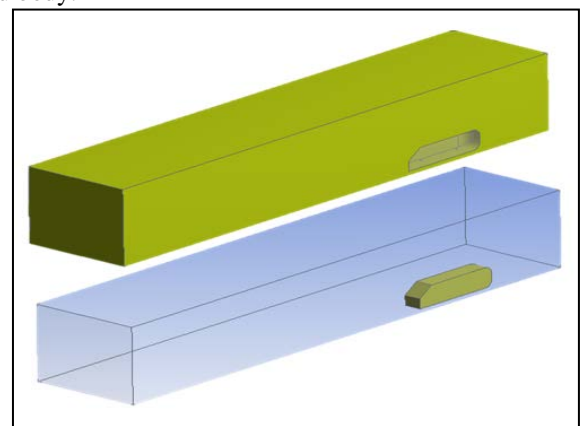


Fig. 7. Boolean operation on Ahmed Body and fluid body

**I. Meshing:**

The length of the first cell away from the surface (y) to calculate effectively the wall shear stress during the simulation should be calculated carefully. To do so, Y+ calculations should be performed to calculate the value of (y) before start meshing process.

1) Reynolds Number (Re):

$$Re = \frac{\rho v l}{\mu} = \frac{\rho l}{\mu} v$$

$$Re = \frac{40 \times 0.288}{15 \times 10^{-6}}$$

$$Re = 768,000$$

2) Skin-Friction Coefficient (Cf):

$$C_f = [2 \log_{10}(Re_x) - 0.65]^{-2.3}$$

for  $Re_x < 10^9$

$$C_f = [2 \log_{10}(768,000) - 0.65]^{-2.3}$$

$$C_f = 3.925 \times 10^{-3}$$

3) Wall Shear Stress ( $\tau_w$ ):

$$\tau_w = C_f \times \frac{1}{2} \rho U_{freestream}^2$$

$$\tau_w = (3.295 \times 10^{-3}) \times \frac{1}{2} \times 1.225 \times 40^2$$

$$\tau_w = 3.847 \text{ Pa}$$

4) Friction Velocity:

$$u^* = \sqrt{\frac{\tau_w}{\rho}}$$

$$u^* = \sqrt{\frac{3.847}{1.225}}$$

$$u^* = 1.772 \text{ m/s}$$

For most near-wall modeling,  $Y^+ \approx 1.0$ . (Salim & Cheah, 2009)

Therefore,

5) Wall Distance (y):

$$y = \frac{y^+ \mu}{\rho u^*}$$

$$y = \frac{1.0 \times (1.789 \times 10^{-5})}{1.225 \times 1.772}$$

$$y = 8.241 \times 10^{-6} \text{ m}$$

Therefore, the boundary layer thickness (wall Distance) for this analysis is  $8.241 \times 10^{-6} \text{ m}$ .

Figure 8 shows screen shots of the final mesh used in the present analysis.

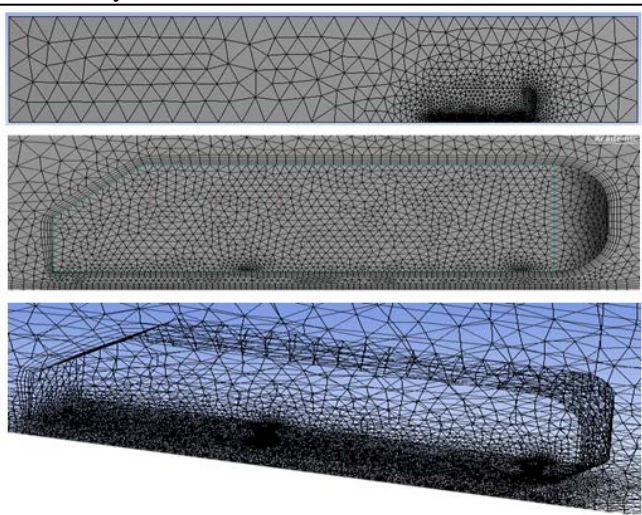


Fig. 8. Screen shots of the final mesh

The maximum number of elements (cells) generated in this grid is about 500,000 cells; since this is the allowable number of cells you can generate using the student license.

**SOLUTION PROCEDURES:**

**J. CFD Model Set-Up:**

Figures 9, 10, and 11 show screen shots of the solution general setting model selection and turbulence model in ANSYS Fluent solver for the investigated flow, respectively.

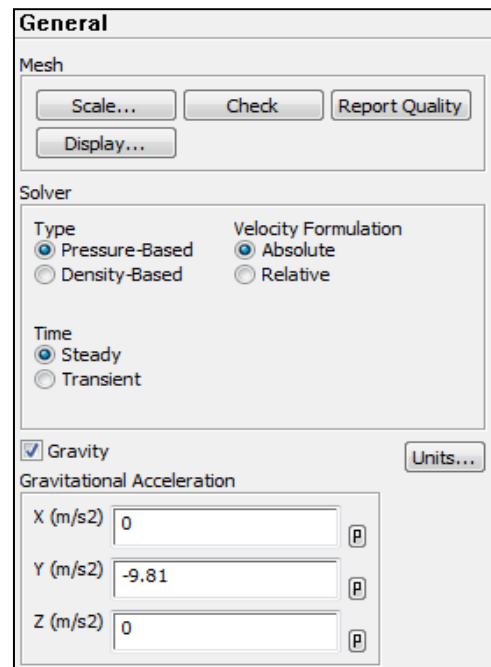


Fig. 9. Solver general setting

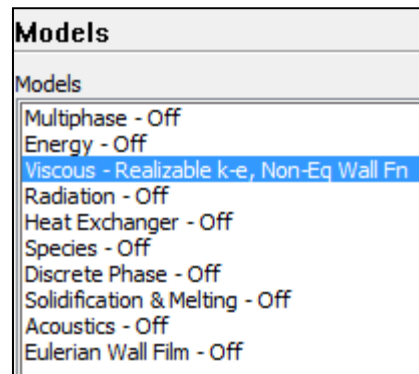


Fig. 10. Model selection

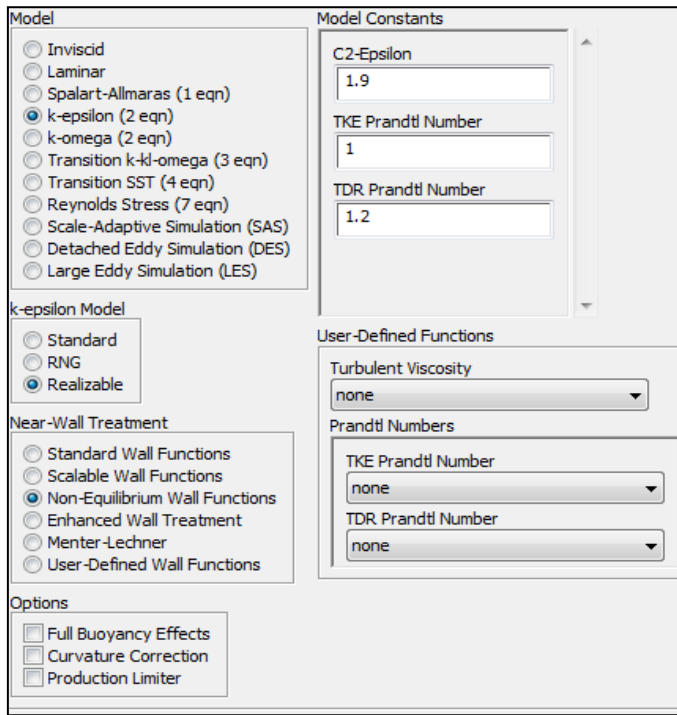


Fig. 11. Turbulent model selection

Figures 12, 13, and 14 show screen shots for the material setting boundary conditions and reference values in ANSYS Fluent solver for the investigated flow respectively.

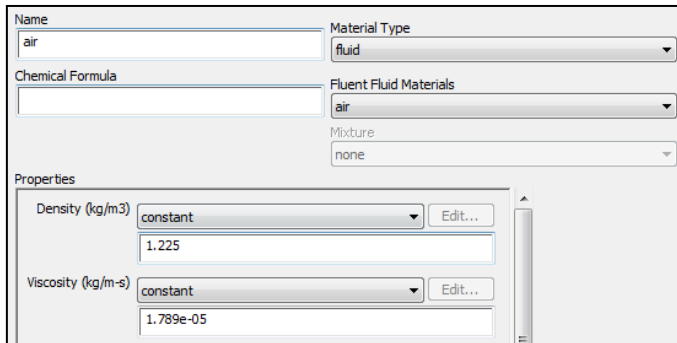


Fig. 12. Air properties

Fig. 13. Boundary Conditions

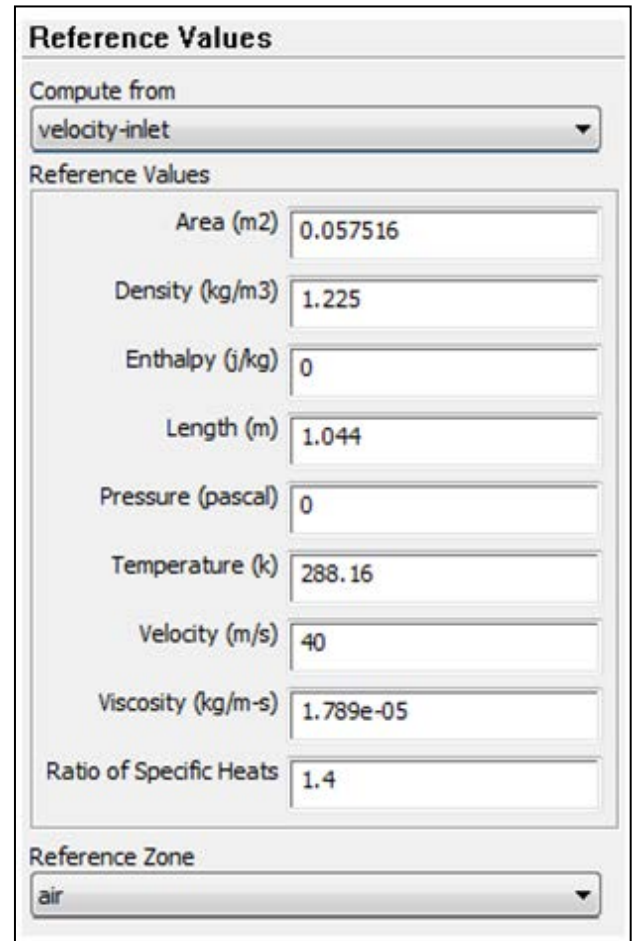


Fig. 14. Reference Values

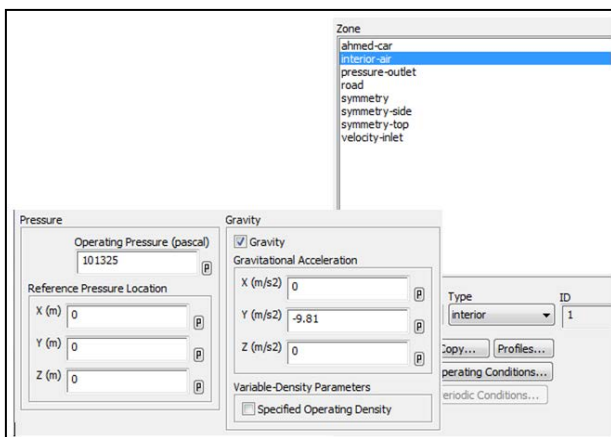
**K. Numerical Schemes:**

The numerical schemes used in the current simulation can be summarized as follows methods:

- Coupled Scheme: This scheme is used for Pressure-Velocity Coupling Method, which enables the full pressure based solver, which has superior performance.
- Least-Squares Cell-Based: This is used for the gradients within the interpolation methods. This scheme has the same accuracy as the node-based gradients, however, is less computationally intensive.
- Second-Order Upwind: The scheme is used for interpolation process, which pressure, momentum and turbulence act upon. This will give better accuracy.

**L. Solution Controls:**

Figures 15, 16 and 17 show screen shots for the solution control residual monitoring and solution initialization, respectively.



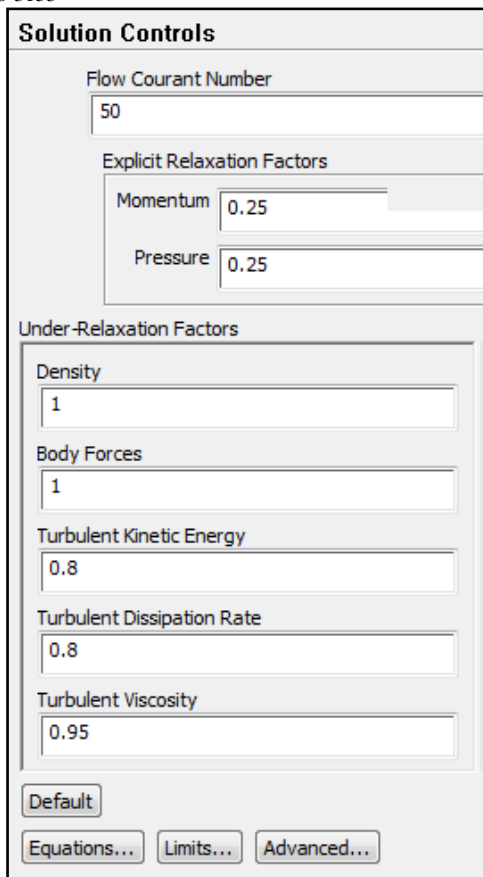


Fig. 15. Solution controls parameters

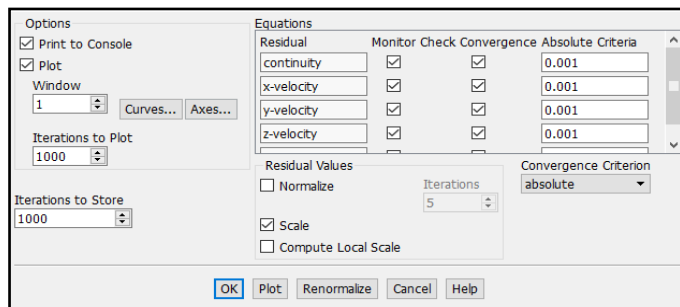


Fig. 16. Residuals monitoring

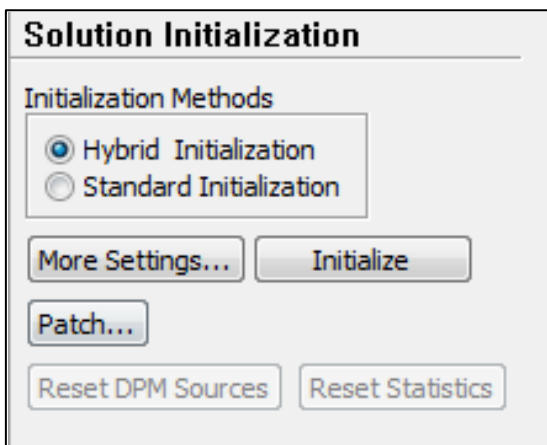


Fig. 17. Solution initialisation

RESULTS ANALYSIS:

*M. Convergence History:*

Figure 18 shows a screen shot from the solution convergence history at about 250 iterations.

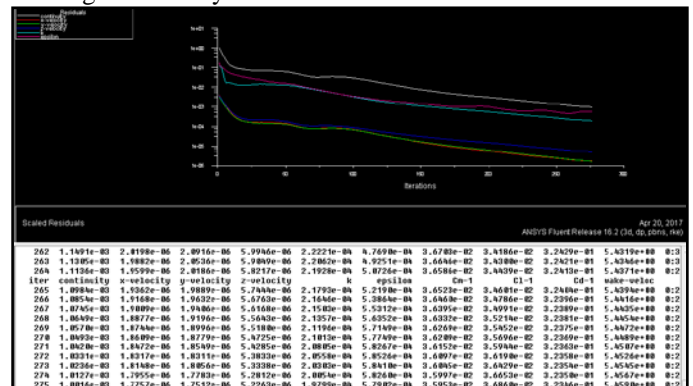


Fig. 18. Convergence history

*N. Static Pressure Contours:*

Figure 19 shows a screen shot of the static pressure contours around Ahmed Body. From the figure, it can be seen that the highest value of static pressure is located at the centre of the oncoming Ahmed body and the minimum value is located the separated flow region.

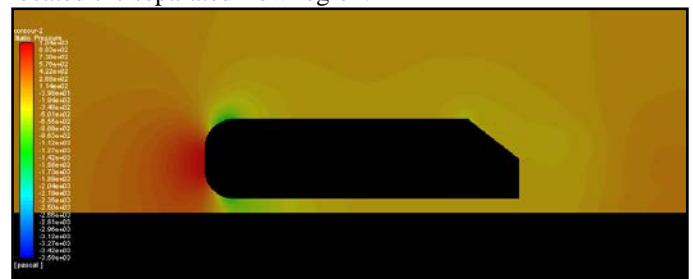


Fig. 19. Static pressure contours

*O. Velocity Magnitude*

Figure 20 shows a screen shot of the velocity magnitude contours around Ahmed Body.

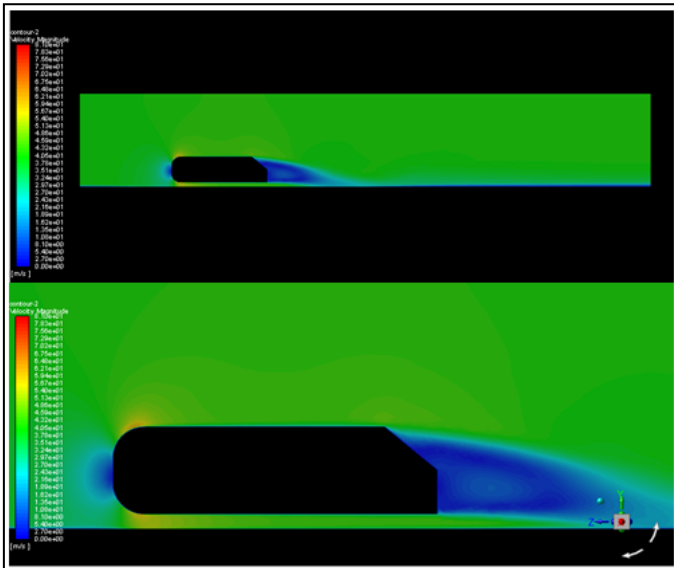


Fig. 20. Velocity magnitude contours

**P. Axial Velocity**

Figure 21 shows a screen shot of the contours of axial velocity component of the flow around Ahmed Body.

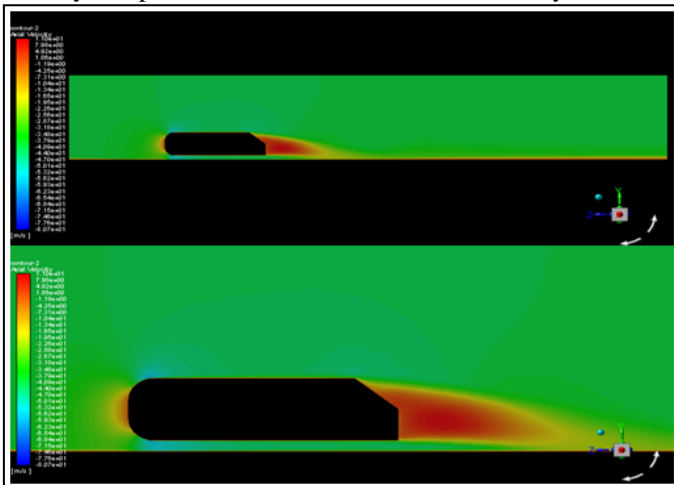


Fig. 21. Axial-velocity contour

**Q. Pressure Coefficient:**

Figure 22 shows a screen shot of the pressure coefficient distribution on the top surface of Ahmed Body.

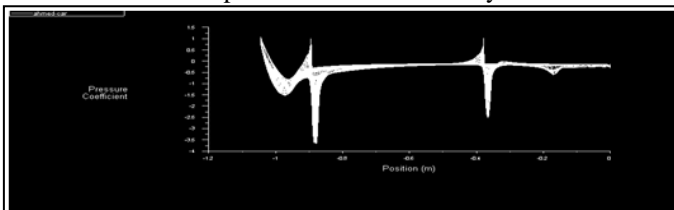


Fig. 22. Pressure coefficient plot

**R. The plot Comparison with Experimental Data**

Table 1 shows the values of the important parameters obtained from the simulation.

TABLE I. VALUES OF THE IMPORTANT PARAMETERS

Outputs	Value
Coefficient of Lift	0.036860
Coefficient of Drag	0.32346
Coefficient of Moments	0.035953
Vertex Average of Velocity Magnitude	5.4590 ms <sup>-1</sup>
K	0.00019799
Epsilon	0.00057902

Table 2, figure 23 and figure 24 show the data from the experiments.

TABLE II. DATA OF THE EXPERIMENTS.

Rear slant angle (°) (In Degrees)	C <sub>d</sub>	C <sub>l</sub>
0	2.50031e-01	-1.17457e-01
5	2.37215e-01	-1.49709e-02
7.5	2.34631e-01	2.92149e-02
10	2.36738e-01	8.29710e-02
12.5	2.41644e-01	1.32483e-01
15	2.46833e-01	1.85001e-01
20	2.61934e-01	2.83622e-01
30	2.97872e-01	3.47783e-01
35	2.94980e-01	2.05502e-01
40	2.50360e-01	8.36791e-01

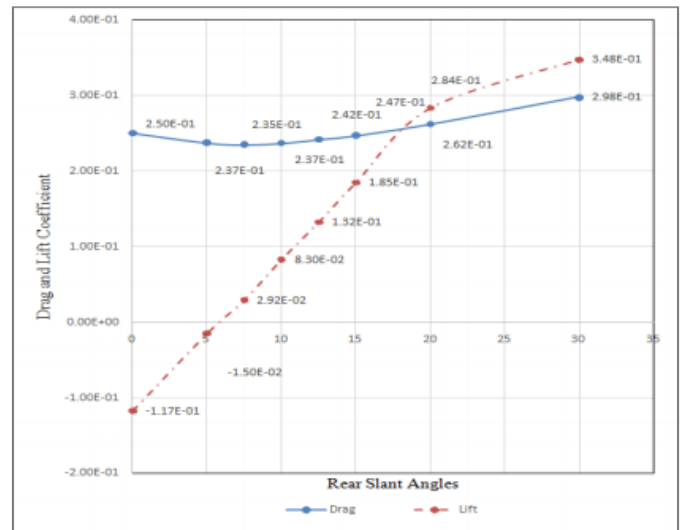


Fig. 23. Experimental CD (Banga, et al., 2015)

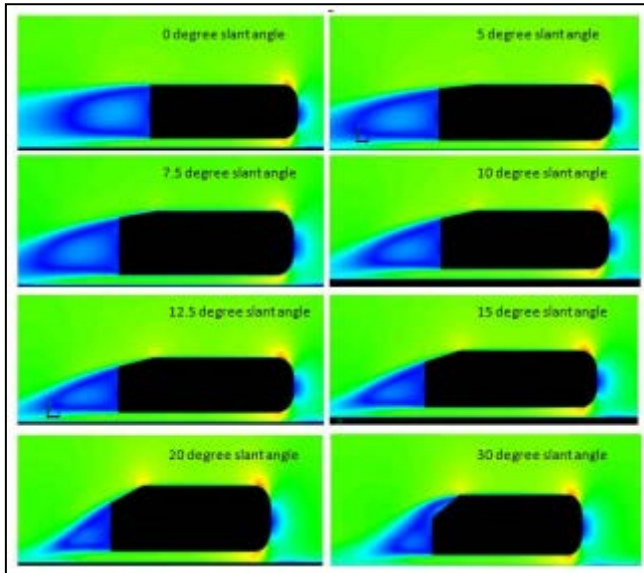


Fig. 24. Experimental velocity magnitude (Banga, et al., 2015)

CONCLUSIONS AND RECOMMENDATIONS

CFD simulation has been carried out to investigate the flow characteristics over a model car (Ahmed Body). The aim was to calculate the aerodynamic coefficients from the CFD simulation and compared them with the available experimental data. The numerical values obtained were;  $CL=0.0368$ ,  $CD=0.323$  and  $CM=0.036$ , respectively. The numerical results are agreed in decent way with experimental data.

REFERENCES

[1] Anderson, J. D. et al., 2009. *Computational Fluid Dynamics: An Introduction*. Berlin: Springer Berlin Heidelberg.  
 [2] ANSYS, 2006. *Modeling Turbulent Flows-Introductory FLUENT Training*. [Online] Available at: [http://www.southampton.ac.uk/~nwb/lectures/GoodPracticeCFD/Articles/Turbulence\\_Notes\\_Fluent-v6.3.06.pdf](http://www.southampton.ac.uk/~nwb/lectures/GoodPracticeCFD/Articles/Turbulence_Notes_Fluent-v6.3.06.pdf) [Accessed 19 April 2017].  
 [3] ANSYS, 2010. *Introduction to ANSYS FLUENT - Lecture 5: Solver Settings*. [Online] Available at: [http://imechanica.org/files/fluvent\\_13.0\\_lecture05-solver-settings.pdf](http://imechanica.org/files/fluvent_13.0_lecture05-solver-settings.pdf) [Accessed 20 April 2017].  
 [4] Banga, S. et al., 2015. CFD Simulation of Flow around External Vehicle: Ahmed Body. *IOSR Journal of Mechanical and Civil Engineering*, 12(4), pp. 87-94.  
 [5] Benson, T., 2014. *Boundary Layer*. [Online] Available at: <https://www.grc.nasa.gov/WWW/BGH/boundlay.html> [Accessed 18 April 2017].  
 [6] Thabit, Thabit H., and Younus, Saif Q., 2018, Risk Assessment and Management in Construction Industries, *International Journal of Research and Engineering*, Vol. 5, No. 2, pp. 315-320.  
 [7] Davis, N., 2015. *FLUENT Lab Exercise 10 - Ahmed Car Body*, Illinois: Computational Science and Engineering Illinois.  
 [8] Dempster, C. M., 2016. *Wind Tunnel Testing of a NACA Aerofoil to Validate CFD Modelling Results Using ANSYS FLUENT*, Pontypridd: University of South Wales.  
 [9] Dobrev, I. & Massouh, F., 2014. *Investigation of Relationship Between Drag and Lift Coefficients for a Generic Car Model*. Sozopol, BULTRANS.

[10] Dumas, L., 2011. *CFD-based Optimization for Automotive Aerodynamics*. Paris: Université Pierre et Marie Curie.  
 [11] Flowmeter Directory, 2017. *Reynolds Number Calculator*. [Online] Available at: [http://www.flowmeterdirectory.com/reynolds\\_calculator.html](http://www.flowmeterdirectory.com/reynolds_calculator.html) [Accessed 18 April 2017].  
 [12] Hewitt, G. F., 2010. *Computational fluid dynamics*. [Online] Available at: <http://www.thermopedia.com/content/279/> [Accessed 13 April 2017].  
 [13] Hinterberger, C., García-Villalba, M. & Rodi, W., 2004. *Large eddy simulation of flow around the Ahmed Body*, Karlsruhe: University of Karlsruhe.  
 [14] Kuzmin, D., 2010. *A Guide to Numerical Methods for Transport Equations*. Nurenburg: Friedrich-Alexander-Universität Erlangen-Nürnberg.  
 [15] Lanfrit, M., 2005. *Best Practice Guidelines for Handling Automotive External Aerodynamics with FLUENT*, Darmstadt: Fluent Deutschland GmbH.  
 [16] Liu, Y. & Moser, A., 2001. *Numerical Modeling of Airflow over the Ahmed Body*, Zentrum: Swiss Federal Institute of Technology.  
 [17] Meile, W. et al., 2011. Experiments and numerical simulations on the aerodynamics of the Ahmed body. *CFD Letters*, 3(1), pp. 32-39.  
 [18] Mohamed, M., 2017. *NG4H246-Further Computational Fluid Dynamics-Car Model Aerodynamics using ANSYS Software Assignment Cover Sheet*, Pontypridd: University of South Wales.  
 [19] Rakshith, K. N. & Mahesh, T. S., 2015. Computations Study of Turbulent Flow around a Generic Car Body (Ahmed Body). *International Journal for Scientific Research and Development*, 3(09), pp. 665-669.  
 [20] Saad, T. & Ragavan, S., 2013. *Historical perspective*. [Online] Available at: [http://www.cfd-online.com/Wiki/Historical\\_perspective](http://www.cfd-online.com/Wiki/Historical_perspective) [Accessed 21 April 2016].  
 [21] Salim, S. M. & Cheah, S. C., 2009. *Wall y+ Strategy for Dealing with Wall-Bounded Turbulent Flows*. Hong Kong, IMECS.  
 [22] Sirius CFD, 2012. *ANSYS Fluent for Vehicle Aerodynamics*. [Online] Available at: <https://www.youtube.com/user/eoescipy/videos> [Accessed 20 April 2017].  
 [23] Sleigh, P. A., 2008. *Laminar and Turbulent Flow*. [Online] Available at: [http://www.efm.leeds.ac.uk/CIVE/CIVE1400/Section4/laminar\\_turbulent.htm](http://www.efm.leeds.ac.uk/CIVE/CIVE1400/Section4/laminar_turbulent.htm) [Accessed 18 April 2017].  
 [24] Thabet, Senan, and Thabit, Thabit H., 2018, Computational Fluid Dynamics: Science of the Future, *International Journal of Research and Engineering*, Vol.5, No. 6, pp. 430-433.  
 [25] Smith, R., 2008. *Car Design and CFD*. [Online] Available at: <http://www.symscape.com/blog/car-design-cfd> [Accessed 13 April 2017].  
 [26] The Engineering ToolBox, 2017. *Laminar, Transitional or Turbulent Flow*. [Online] Available at: [http://www.engineeringtoolbox.com/laminar-transitional-turbulent-flow-d\\_577.html](http://www.engineeringtoolbox.com/laminar-transitional-turbulent-flow-d_577.html) [Accessed 18 April 2017].  
 [27] Visavale, G., 2006. *Reviewing Governing Equations of Fluid Dynamics*. [Online] Available at: <https://www.learncax.com/knowledge-base/blog/by-category/cfd/reviewing-governing-equations-of-fluid-dynamics> [Accessed 20 April 2017].

